Autoregressive processes with exponentially decaying probability distribution functions: Applications to daily variations of a stock market index

Markus Porto[1] and H. Eduardo Roman[2]
[1]*Max-Planck-Institut für Physik komplexer Systeme, Nöthnitzer Straße 38, 01187 Dresden, Germany*
[2]*Dipartimento di Fisica and INFN, Università di Milano, Via Celoria 16, 20133 Milano, Italy*
(Received 13 November 2001; revised manuscript received 23 January 2002; published 11 April 2002)

We consider autoregressive conditional heteroskedasticity (ARCH) processes in which the variance σ_y^2 depends *linearly* on the absolute value of the random variable y as $\sigma_y^2 = a + b|y|$. While for the standard model, where $\sigma_y^2 = a + by^2$, the corresponding probability distribution function (PDF) $P(y)$ decays as a power law for $|y| \to \infty$, in the linear case it decays exponentially as $P(y) \sim \exp(-\alpha|y|)$, with $\alpha = 2/b$. We extend these results to the more general case $\sigma_y^2 = a + b|y|^q$, with $0 < q < 2$. We find stretched exponential decay for $1 < q < 2$ and stretched Gaussian behavior for $0 < q < 1$. As an application, we consider the case $q = 1$ as our starting scheme for modeling the PDF of daily (logarithmic) variations in the Dow Jones stock market index. When the history of the ARCH process is taken into account, the resulting PDF becomes a stretched exponential even for $q = 1$, with a stretched exponent $\beta = 2/3$, in a much better agreement with the empirical data.

DOI: 10.1103/PhysRevE.65.046149 PACS number(s): 02.50.Ey, 05.40.Fb, 87.23.Ge

I. INTRODUCTION

Extensively employed in finance today, autoregressive conditional heteroskedasticity (ARCH) processes have been constructed to mimick the (often quite strong) variable volatility of stock prices, by letting the variance of the random process being a function of the random variable itself [1,2]. Interestingly, ARCH processes are characterized by power-law tails in the associated probability distribution functions (PDF's) [3–5]. Since power laws are widespreadly observed also in natural science phenomena [6], the applicability of ARCH processes to such fields as physics and biology can thus be expected to grow in popularity in coming years. Despite the ubiquitous character of power-law decay in several physical and natural science problems, a variety of exponentially decaying distribution functions, ranging from stretched exponential (see, e.g., Ref. [7]) to stretched Gaussian decay (see, e.g., Ref. [8]), are also observed which, in most cases, are a result of long-range correlations in the system. The question we wish to address here is how such different types of exponentially decaying distributions can be modeled within the context of short-range correlations, as for instance in the case of ARCH processes, and how can they be implemented for describing stock market behavior.

The paper is organized according to the following lines. In Sec. II, we briefly recall the definition and simplest version of an ARCH process, and discuss how it can be modified to yield exponentially decaying PDF's. Secondly, we generalize the ARCH model to the case of stretched exponential and stretched Gaussian PDF's. In Sec. III, we apply the results of the preceding section to financial data, aiming at describing the daily variations of a stock market index, in particular, of the Dow Jones Industrial Average (DJIA) within the period from 1928 to 2001. The comparison between the empirical data and the model predictions indicates that the latter do not display all the characteristic aspects of the market, in particular, the long-range correlations of absolute returns (or volatility). This suggests us that the missing feature of the model may be hidden in the ''history'' of the process itself, and should be taken into account. This is achieved by calculating, at each step n, the standard deviation

$$\sigma_T(n) = (\langle x^2 \rangle_T - \langle x \rangle_T^2)^{1/2} \tag{1}$$

over the previous T values of the process, $\{x_{n-1}, \ldots, x_{n-T}\}$. The quantity $\sigma_T(n)$ is used, together with x_{n-1}, to generate the next value x_n, from a standard distribution. The original standard ARCH process corresponds to the case $T = 1$, i.e., $\sigma_1(n) \equiv 0$. Here we use $T = 700$ steps, aimed at fitting the present data for the DJIA, where volatility correlations persist up to a time horizon of about 700 trading days (i.e., ≈ 3 yr). Incorporating a history in the model makes it non-Markovian, but it still remains simpler than the extensively employed generalized ARCH (GARCH) processes, in which the variance is a function of several of its previous values [9]. Finally, Sec. IV is devoted to the summary of our main results and conclusions.

II. ARCH(1) PROCESSES AND THEIR GENERALIZATIONS

Let us consider the simplest case, i.e., an ARCH(1) process [1]. It is defined as an iterative map of the form $x_n = \mathcal{R}(x_{n-1})$, where the outcome x_n, after the nth iteration step, depends only on its previous value x_{n-1}, and $\mathcal{R}(y)$ is a random process. The latter is completely specified by the transition probability distribution function $W(y \curvearrowright x)$, generally assumed to be a Gaussian distribution,

$$W(y \curvearrowright x) \equiv \frac{1}{\sqrt{2\pi\sigma_y^2}} \exp\left(-\frac{x^2}{2\sigma_y^2} \right), \tag{2}$$

obeying the normalization condition $\int_{-\infty}^{\infty} dx\, W(y \curvearrowright x) = 1$. For standard ARCH(1) processes, $\sigma_y^2 = a + by^2$, where $a > 0$ and $b \geqslant 0$ are the model parameters. In this case, the average

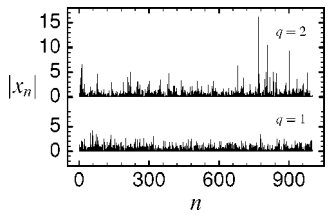

FIG. 1. A sequence of random numbers x_n, plotted as $|x_n|$ vs n, generated according to ARCH(1) rules, for a standard ARCH(1) process with $\sigma_y^2=a+by^2$ $(q=2)$ and for an ARCH(1) process with $\sigma_y^2=a+b|y|$ $(q=1)$. In both cases we used $a=0.4$ and $b=0.99$, yielding a mean variance $\sigma^2=40$ for $q=2$ and $\sigma^2\approx 1.25$ for $q=1$, respectively.

variance is $\langle\sigma^2\rangle=a/(1-b)$. It can be shown that the PDF $P(x)$ for ARCH(1) processes satisfies the self-consistent equation [1,3,5]

$$P(x)=\int_{-\infty}^{\infty} dy\, W(y\curvearrowright x)\, P(y), \tag{3}$$

which decays as a power law, $P(x)\sim|x|^{-\alpha}$, for $|x|\to\infty$, with α related to the parameter b by $b^{-(\alpha-1)/2}=2^{(\alpha-1)/2}\Gamma(\alpha/2)/\sqrt{\pi}$ [3,5] (see also [4]). Clearly, if $b=0$, the process reduces to a standard one and $P(x)=G(x)\equiv(2\pi a)^{-1/2}\exp(-x^2/2a)$.

Since the quadratic dependence of $\sigma_y^2=a+by^2$ on y gives rise to a power-law decay of $P(x)$, the question is whether a weaker dependence, for instance, the linear relation

$$\sigma_y^2\equiv a+b|y|, \tag{4}$$

may have associated a faster decaying PDF. Here, we show that this is indeed the case, the corresponding PDF decays exponentially as

$$P(x)\sim\exp(-\alpha|x|), \quad \text{when } |x|\to\infty, \tag{5}$$

and our aim is to calculate the value of α exactly. Before doing that, it is illustrative to visualize the behavior of series of random numbers x_n, by plotting, for instance, their absolute values $|x_n|$ as a function of n, for the standard and linear cases, respectively, as shown in Fig. 1. Such series not only resemble very much the empirically observed variable volatility of stock prices, but may well find interesting applications in a variety of physical processes.

Let us consider now the calculation of the decay rate α. Following the approach employed in Ref. [5], we consider that in the limit of large $|x|$, the integrand in Eq. (3) is dominated by large values of $|y|$ and one can replace Eq. (4) by $\sigma_y^2=b|y|$. Using the exponential ansatz $P(y)\sim\exp(-\alpha|y|)$ within the integrand of Eq. (3), the calculation reduces to the convolution

$$\exp(-\alpha|x|)=\frac{2}{\sqrt{2\pi}}\int_0^{\infty}\frac{dy}{\sqrt{by}}\exp(-x^2/[2by])\exp(-\alpha y), \tag{6}$$

which can be performed exactly (see, e.g., Ref. [10]) to yield

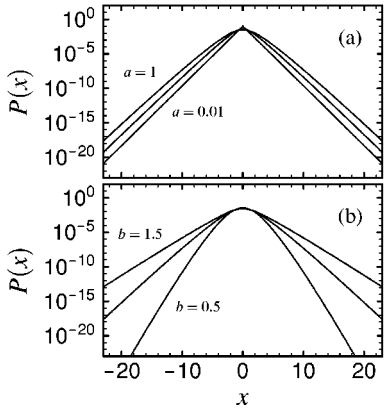

FIG. 2. The PDF $P(x)$ vs x for ARCH(1) processes with variable variance $\sigma_y^2=a+b|y|$ (see text for details). (a) $b=1$ for $a=1$ (top), 0.4, and 0.01 (bottom). For $a=0.01$, the numerical results almost coincide with the exact solution, Eq. (8). (b) $a=1$ for $b=0.5$ (bottom), 1, and 1.5 (top).

$$\exp(-\alpha|x|)=\sqrt{\frac{2}{\alpha b}}\exp(-\sqrt{2\alpha/b}|x|). \tag{7}$$

The equality holds when the prefactor $\sqrt{2/\alpha b}=1$ and we find $\alpha=2/b$. To be noted is that the above exponential decay actually corresponds to the exact shape of the PDF in the case that $a=0$, which in this particular case reads

$$P(x)=\frac{1}{b}\exp(-2|x|/b), \tag{8}$$

yielding a mean variance $\sigma^2=b^2/2$ and a finite kurtosis $\kappa\equiv\langle x^4\rangle/\sigma^4=6$. Note that $P(x)$ obeys the exact scaling relation, $\sigma P(y)=(1/\sqrt{2})\exp(-\sqrt{2}y)$, with $y=|x|/\sigma$. When $a>0$, $P(x)$ departs from the analytical result Eq. (8). Some numerical examples are reported in Fig. 2 for different values of a and b.

In what follows, we extend the previous results by showing that for $|x|\to\infty$ different exponential decays of the type

$$P(x)\sim\exp(-\alpha|x|^{\beta}), \tag{9}$$

with $0<\beta<2$, can be obtained within ARCH(1) processes by generalizing Eq. (4) to the form

$$\sigma_y^2\equiv a+b|y|^q, \tag{10}$$

where $0<q<2$. The cases with $0<\beta<1$ correspond to stretched exponential decay, while those with $1<\beta<2$ to stretched Gaussian behavior. Assuming the asymptotic form Eq. (9) for $P(x)$, Eq. (6) becomes

$$\exp(-\alpha|x|^{\beta})\sim\frac{2}{\sqrt{2\pi}}\int_0^{\infty}\frac{dy}{\sqrt{by^q}}\exp(-x^2/[2by^q])\times\exp(-\alpha\ y^{\beta}). \tag{11}$$

The leading asymptotic behavior of the integral, when $|x|\to\infty$, can be obtained analytically by the saddle-point method. The saddle occurs at

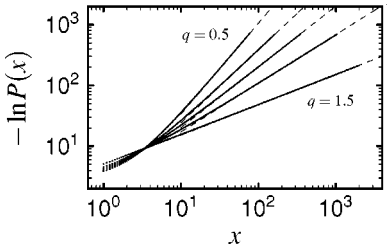

FIG. 3. The asymptotic decay of the PDF $P(x)$, plotted as $-\ln P(x)$ vs x (>0), for ARCH(1) processes with variable variance $\sigma_y^2=a+b|y|^q$, when $a=0.01$ and $b=1$ for the cases: $q=1.5$ (bottom), $q=1.2$, $q=1.0$, $q=0.8$, and $q=0.5$ (top). The dashed lines correspond to the generalized exponential decays expected from Eqs. (9) and (14).

$$y_*=\left(\frac{qx^2}{2b\alpha\beta}\right)^{1/(q+\beta)}, \tag{12}$$

and we find

$$\exp(-\alpha|x|^\beta)\sim\exp(-A|x|^{2\beta/(q+\beta)}), \tag{13}$$

where $A=[(q+\beta)/(2b)](2b\alpha\beta/q)^{q/(q+\beta)}$. Thus, according to Eq. (13), we obtain the relations $\beta=2\beta/(q+\beta)$ and $A=\alpha$, yielding

$$\beta=2-q \quad \text{and} \quad \alpha=\frac{1}{b}\left(\frac{2}{q}(2-q)\right)^{q/(2-q)}, \tag{14}$$

which reduce to the previously discussed results when $q=1$ (i.e., simple exponential decay), where $\beta=1$ and $\alpha=2/b$. We have verified the validity of the theoretical predictions, Eq. (14), by extensive numerical simulations. Some illustrative examples are displayed in Fig. 3.

Let us consider finally the more general case in which the parameter b may change at each iteration step, in such a way that it fluctuates according to the normal distribution $G(b)=(8\pi\hat{b}^2)^{-1/2}\exp[-b^2/(2\hat{b}^2)]$, for $b\geqslant 0$, with a constant width $\hat{b}$. The resulting PDF will now be given by the convolution

$$\hat{P}_{\rm con}^{(q)}(x)\sim\int_0^\infty dbG(b)\exp(-\alpha|x|^\beta), \tag{15}$$

with α and β given in Eq. (14). The integral can be evaluated using the saddle-point method, yielding the asymptotic behavior

$$\hat{P}_{\rm con}^{(q)}(x)\sim\exp\left[-\frac{3}{2}\hat{\alpha}_q^{2/3}\left(\frac{|x|}{\hat{b}}\right)^{2\beta/3}\right], \tag{16}$$

where $\hat{\alpha}_q=\hat{b}^{\beta-1}(2\beta/q)^{q/\beta}$.

In the following, we argue that these generalized ARCH processes, with $0<q<2$, can suitably describe stock market data and may be considered a useful alternative to the widely used ARCH or GARCH processes [1,9], corresponding to the single case $q=2$.

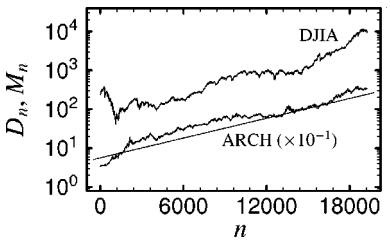

FIG. 4. Dow Jones Industrial Average (DJIA) D_n vs trading day n, within the period from October 1928 to May 2001 (upper line). The results for the present ARCH model M_n Eq. (23), have been shifted downwards for clarity. The straight line corresponds to a constant bias growth, $\exp(\mu n)$ with $\mu=1.9531\times10^{-4}$, and is shown for illustration.

III. APPLICATION TO DAILY STOCK MARKET DATA

To this end, let us consider financial data from the New York Stock Exchange, represented by the daily closing values of the DJIA in the period from 1928 to 2001. The DJIA values D_n are displayed by the continuous (top) line in Fig. 4, as a function of the trading day n. Also included in the plot are the results of model calculations and a straight line as explained below.

In the following, we wish to characterize the empirical data by calculating the PDF of the day-to-day variations of D_n. For convenience, we consider the relative variations of the index by calculating the differences of their logarithms as

$$y_n=\ln D_n-\ln D_{n-1}, \tag{17}$$

from which we obtain the corresponding PDF $P(y)$. The resulting variance is $\sigma_{\rm DJIA}^2=\langle y^2\rangle-\langle y\rangle^2=1.2312\times10^{-4}$. Note that due to the long-term growth rate (cf. Fig. 4), the mean value $\langle y\rangle=1.9531\times10^{-4}>0$, yet it is still small as compared to $\sigma_{\rm DJIA}=1.11\times10^{-2}$. The PDF $P(y)$ is displayed by the full circles in Fig. 5, the latter seem to follow a simple exponential shape near the center of the distribution. A closer inspection of the data indicates, however, that the actual shape deviates from the pure exponential one, and other functional dependencies may fit the data better. At any rate, this result tells us that an exponential decay is already a good approximation to the shape of $P(y)$ and the models described in the preceding section may be appropriate in this case.

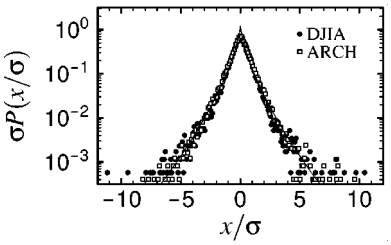

FIG. 5. Scaling plot of the PDF $P(x)$, plotted as $\sigma P(x)$ vs x/σ for the DJIA (full circles) and the ARCH model results [open squares, cf. Fig. 4 and Eq. (23)], both based on similar statistics. The continuous line represents the analytical form, Eq. (25).

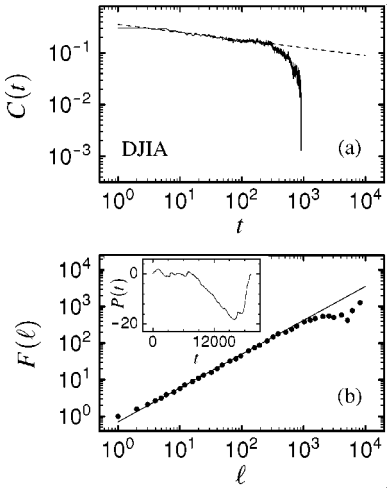

FIG. 6. Correlations of absolute returns for the DJIA. (a) Autocorrelation function $C(t)$ vs time lag t, Eq. (19), where $\langle|y|\rangle = 7.110\times10^{-3}$ and $\langle|y|^2\rangle = 1.229\times10^{-4}$. The graph has been truncated at the first node of $C(t)$. The dashed line represents the behavior $C(t)\sim t^{-\kappa}$ and has the slope $\kappa=0.15$. (b) Fluctuation analysis: Fluctuation function $F(\ell)$ vs time scale ℓ for the random walk profile $P(t)$ (shown in the inset). The continuous line displays the behavior $F(\ell)\sim\ell^{\nu}$, with $\nu=0.925$. Note that ν and κ are related to each other by $\kappa=2-2\nu$.

We have, therefore, considered an ARCH(1) process [cf. Eq. (4)] as our starting point for modeling the DJIA, and first incorporated a constant bias rate, $\mu=1.9531\times10^{-4}$, in order to simulate the exponential growth observed for the empirical data (the straight line in Fig. 4). Specifically, we have obtained a sequence x_n, using Eq. (4), and constructed the daily index model M_n in the form

$$M_n = M_0 \exp\left(\sum_{i=1}^{n} x_i\right)\exp(\mu n). \tag{18}$$

Hence, we have the correspondence $M_n \to D_n$ and $x_n+\mu \to y_n$. The PDF is now centered at μ, but the effect of the bias term is expected to be small, yielding a negligible shift of $P(x)$.

Two points can be raised now. The first is that by construction, this simple ARCH model yields an exponentially decaying PDF, but as we have seen such a prediction is not conclusively obeyed by the DJIA. A second observation regards the correlations of the absolute returns for the DJIA, represented, e.g., by the autocorrelation function

$$C(t) = \frac{\langle|y_n||y_{n+t}|\rangle - \langle|y|\rangle^2}{\langle|y|^2\rangle - \langle|y|\rangle^2}, \tag{19}$$

results that are plotted in Fig. 6(a). They indicate the existence of long-range correlations in the absolute returns for the DJIA, consistent with other studies reported in the literature (see, e.g., Liu *et al.* in Ref. [2]). The abrupt decay at around $T=1000$ may be a finite size effect, due to the limited number of data considered, and persistence over longer time scales cannot be excluded *a priori*. For our present purposes, however, we will consider that a crossover takes place at around $T=700$.

The temporal behavior of the autocorrelation function $C(t)$ can be identified independently of Eq. (19) by looking at the scaling behavior of the corresponding random walk "profile" $P(t)$, defined as

$$P(t) = \sum_{i=1}^{t} [|y_i| - \langle|y|\rangle]. \tag{20}$$

The "roughness" of the profile tells us about the presence or absence of correlations in the stochastic series. It can be determined quantitatively by calculating the fluctuations of $P(t)$ within a window (time scale) of width ℓ as

$$F(\ell) = \langle[P(t) - P(t+\ell)]^2\rangle^{1/2}, \tag{21}$$

(see, e.g., [11], and Liu *et al.* in Ref. [2] for more details). It is well known that if the autocorrelation function decays as $C(t)\sim t^{-\kappa}$, within a given time scale, with $\kappa<1$, the fluctuations of the profile, Eq. (21), display the power-law behavior $F(\ell)\sim\ell^{\nu}$, where $\nu=1-\kappa/2$, within the same time scale. Note that for $\kappa\geqslant1$, ν sticks at its standard value $\nu=1/2$, describing a simple diffusive behavior characterized by short-range correlations. An example of the latter is also the case of exponentially decaying correlations, $C(t)\sim\exp(-at)$, yielding again $\nu=1/2$ for $F(\ell)$. The method based on Eqs. (20) and (21) has been extensively used in different context, ranging from financial data (as by Liu *et al.* in Ref. [2]) to temperature fluctuations in the atmosphere [11].

The results of the fluctuation analysis, Eq. (21), for the DJIA are reported in Fig. 6(b), yielding a power-law behavior $F(\ell)\sim\ell^{\nu}$, over almost three decades, consistent with the value $\nu=1-\kappa/2=0.925$ expected from the results shown in Fig. 6(a), where $\kappa\approx0.15$. These results can be confronted with the corresponding behavior of the simple linear ARCH process, Eq. (4), displayed in Fig. 7. As is apparent from Fig. 7(a), the Markovian character of the ARCH process gives rise to an exponentially decaying autocorrelation function, consistent with a fluctuation function growing in the standard diffusive fashion with time scale, $F(\ell)\sim\ell^{1/2}$ [cf. Fig. 7(b)]. We notice that all the model variants discussed in Sec. II behave similarly. Clearly, our simple ARCH process, Eq. (4), needs to be modified.

To do this, we allow next the parameter b to fluctuate as the process evolves. We have found that the simple choice

$$b \to b_{\rm eff}(n) = b_0 + c\,\sigma_T(n)\,T^{-1/2}, \tag{22}$$

where b_0, c, and T are constants, with $\sigma_T(n)$ given in Eq. (1), yields satisfactory results as we will see in the following. The factor $T^{-1/2}$ in Eq. (22) is introduced to compensate the growth $\sigma_T(n)\sim T^{1/2}$, when $T\gg1$, thus making the fluctuations scale invariant. In Eq. (22), b_0 represents the lower cutoff for $b_{\rm eff}(n)$, while $\sigma_T(n)$ is responsible for its fluctuations, calculated within the time horizon T, for a single "trajectory" or realization of the process. Notice that in this way,

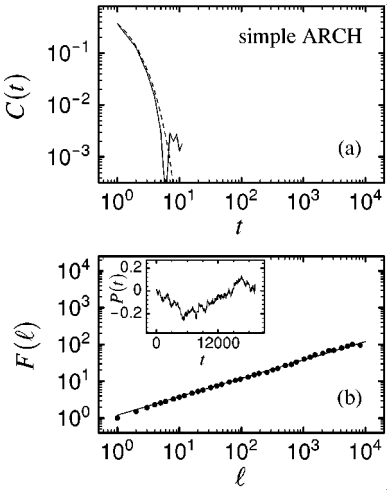

FIG. 7. Same as in Fig. 6 for the simple ARCH process in Eq. (4). (a) Autocorrelation function: $C(t)$ decays exponentially as indicated by the dashed line representing the function $C(t)=\exp(-t)$. (b) Fluctuation analysis: The random walk profile $P(t)$ is now consistent with a standard random walk behavior, i.e., $F(\ell)\sim\ell^{1/2}$ and the straight line has slope $\nu=1/2$.

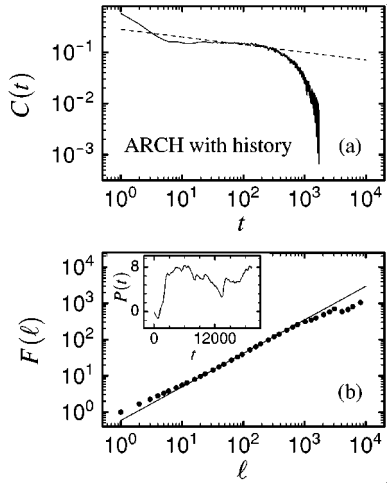

FIG. 8. Same as in Fig. 6 for the ARCH process with history, Eq. (23). (a) Autocorrelation function: The dashed line has the slope $\kappa=0.15$ as in Fig. 6(a), and is shown as a guide. (b) Fluctuation analysis: The random walk profile $P(t)$ displays long-range correlations. The straight line has been drawn as a guide and has slope $\nu=0.925$, as in Fig. 6(b).

the parameter $b_{\rm eff}$ is controlled by the ARCH process itself, thus keeping the number of relevant parameters in the model essentially unchanged.

We then suggest the following ARCH model for describing the daily DJIA data in the form $y_n=x_n+\mu$ (with $\mu=1.9531\times10^{-4}$ for the period 1928–2001), where $x_n=\mathcal{R}_\sigma(x_{n-1})$. The random process $\mathcal{R}_\sigma$ obeys the transition probability distribution function $W(x_{n-1}\frown x_n)$ given in Eq. (2), with

$$\sigma_n^2=a+b_{\rm eff}(n)|x_{n-1}| \quad \text{and}$$

$$b_{\rm eff}(n)=b_0+c\sigma_T(n)T^{-1/2}, \tag{23}$$

where $a=10^{-6}$, $b_0=2\times10^{-3}$, $c=2.74$, $T=700$, and $\sigma_T(n)$ is given by Eq. (1). The resulting values $M_n=M_0\exp(\Sigma_{i=1}^n x_i)\exp(\mu n)$, for $M_0=30$ and $1\leqslant n\leqslant20000$, are plotted in Fig. 4, where they can be compared with the DJIA data. The corresponding PDF $\hat{P}(x)$ is displayed by the open squares in Fig. 5, in very good agreement with the full circles for the DJIA. The associated autocorrelation and fluctuation functions are reported in Fig. 8, in good agreement with the empirical data. In this plot, the length of the series used was 10 times longer than that of the DJIA in order to avoid finite size effects. If the same number of points ($N\approx20\,000$) is used, $C(t)$ goes to zero already at $t\approx900$. Interestingly, for larger values of the cutoff T ($\gg700$), $C(t)$ becomes independent of T for $t\ll T$.

It is illustrative to note that $\hat{P}(x)$ can be estimated in an approximate way from the convolution [cf. Eq. (15)]

$$\hat{P}_{\rm con}(x)\approx\int_0^\infty dbG(b)P_b(x), \tag{24}$$

where $P_b(x)$ is given by Eq. (8), while the values of b are assumed to be normally distributed on long time scales as, $G(b)=(8\pi\hat{b}^2)^{-1/2}\exp[-b^2/(2\hat{b}^2)]$, $b\geqslant0$, with a width $\hat{b}$ characteristic of the time span T (see above). The asymptotic behavior of $\hat{P}_{\rm con}(x)$ can be obtained by the saddle-point method, yielding $\hat{P}_{\rm con}(x)\sim\exp(-6[|x|/(4\hat{b})]^{2/3})$, which corresponds to the case $q=1$ in Eq. (16). Assuming that the latter holds for all x, the following scaling form for $\hat{P}_{\rm con}(x)$ is obtained:

$$\sigma\hat{P}_{\rm con}(y)=\sqrt{\frac{35}{6\pi}}\exp(-\gamma y^{2/3}), \quad \text{with } y=|x|/\sigma, \tag{25}$$

where $\sigma^2=(35/36)\hat{b}^2$ and $\gamma=(105)^{1/3}/2$. The analytical form Eq. (25) is in excellent agreement with the numerical results for $\hat{P}(x)$ as is apparent from Fig. 5. The stretched exponential decay with $\beta=2/3$ [Eq. (25)] corresponds to the case $q=4/3$ in Eq. (10). Although both processes, Eq. (23) and Eq. (10), have identically decaying PDF's, they display, respectively, long-range and short-range correlations in the absolute returns.

IV. CONCLUSIONS

We have discussed generalizations of the well known ARCH(1) processes, originally introduced in finance, for which the corresponding probability distribution functions display general exponential decay, ranging from stretched exponential to stretched Gaussian behavior. We apply these models to the description of daily changes of a stock market index, such as the Dow Jones Industrial Average. The results suggest that a history of the process is, however, required to simulate the empirical data in a more realistic way, yielding

a process which is no longer Markovian. Despite this complication, the model remains simple and, therefore, attractive to be used in standard Monte Carlo simulations of long-term market scenarios. In addition to such obvious applications in the financial context, these generalized ARCH processes incorporating history may turn out to be appropriate for modeling a broad spectrum of stochastic phenomena in natural and physical sciences.

[1] R.F. Engle, Econometrica **50**, 987 (1982); R.F. Engle and T.P. Bollerslev, Econometric Rev. **5**, 1 (1986); F.X. Diebold, *Empirical Modelling of Exchange Rate Dynamics* (Springer Verlag, New York, 1988); T. Bollerslev, R. Engle, and D. Nelson, *ARCH Models*, in *Handbook of Ecometrics* (North-Holland, Amsterdam, 1993), Vol. IV; R. Engle, *ARCH, Selected Readings* (Oxford University, Oxford, 1995); C. Gouriéroux, *ARCH Models and Financial Applications* (Springer Series in Statistics, New York, 1997).

[2] R.N. Mantegna and H.E. Stanley, Nature (London) **376**, 46 (1995); M.H.R. Stanley, L.A.N. Amaral, S.V. Buldyrev, S. Havlin, H. Leschhorn, P. Maass, M.A. Salinger, and H.E. Stanley, *ibid.* **379**, 804 (1996); Y.K. Lee, L.A.N. Amaral, D. Canning, M. Meyer, and H.E. Stanley, Phys. Rev. Lett. **81**, 3275 (1998); Y. Liu, P. Gopikrishnan, P. Cizeau, M. Meyer, C.-K. Peng, and H.E. Stanley, Phys. Rev. E **60**, 1390 (1999); V. Plerou, P. Gopikrishnan, L.A.N. Amaral, M. Meyer, and H.E. Stanley, *ibid.* **60**, 6519 (1999); M. Pasquini and M. Serva, Econ. Lett. **65**, 275 (1999); Eur. Phys. J. B **16**, 195 (2000); B. Podobnik, P.C. Ivanov, Y. Lee, A. Chessa, and H.E. Stanley, Europhys. Lett. **50**, 711 (2000); P.C. Ivanov, B. Podobnik, Y. Lee, and H.E. Stanley, Physica A **299**, 154 (2001).

[3] L. de Haan, S.I. Resnick, H. Rootzen, C.G. de Vries, Stochastic Proc. Appl. **32**, 213 (1989); P. Embrechts, C. Klüppelberg, and T. Mikosch, *Modelling Extremal Events for Insurance and Finance* (Springer Verlag, Heidelberg, 1999).

[4] D. Sornette, Physica A **250**, 295 (1998).

[5] H.E. Roman and M. Porto, Phys. Rev. E **63**, 036128 (2001); H.E. Roman, M. Porto, and N. Giovanardi, Eur. Phys. J. B **21**, 155 (2001).

[6] C.J. Rhodes and R.M. Anderson, Nature (London) **381**, 600 (1996); P.C. Ivanov, M.G. Rosenblum, C.K. Peng, J. Mietus, S. Havlin, H.E. Stanley, and A.L. Goldberger, *ibid.* **383**, 323 (1996); G.B. West, J.H. Brown, and B.J. Enquist, Science **276**, 122 (1997); N.V. Dokholyan, S.V. Buldyrev, S. Havlin, and H.E. Stanley, Phys. Rev. Lett. **79**, 5182 (1997); N.V. Dokholyan, S.V. Buldyrev, S. Havlin, and H.E. Stanley, J. Theor. Biol. **202**, 273 (2000); L.A.N. Amaral, S.V. Buldyrev, S. Havlin, M.A. Salinger, and H.E. Stanley, Phys. Rev. Lett. **80**, 1385 (1998); G.M. Viswanathan, S.V. Buldyrev, S. Havlin, M.G.E. da Luz, E.P. Raposo, and H.E. Stanley, Nature (London) **401**, 911 (1999); A.L. Barabasi and R. Albert, Science **286**, 509 (1999); J.R. Banavar, A. Maritan, and A. Rinaldo, Nature (London) **399**, 130 (1999); J. Doyle and J.M. Carlson, Phys. Rev. Lett. **84**, 5656 (2000); R. Albert, H. Jeong, and A.L. Barabasi, Nature (London) **406**, 378 (2000).

[7] W. Götze and L. Sjogren, Rep. Prog. Phys. **55**, 241 (1992); J.C. Phillips, *ibid.* **59**, 1133 (1996); K. L. Ngai, in *Disorder Effects on Relaxational Properties*, edited by R. Richert and A. Blumen (Springer, Berlin, 1994).

[8] S. Havlin and D. Ben-Avraham, Adv. Phys. **36**, 695 (1987); A. Bunde, S. Havlin and H.E. Roman, Phys. Rev. A **42**, 6274 (1990); *Fractals and Disordered Systems*, edited by A. Bunde and S. Havlin, 2nd ed. (Springer, Heidelberg, 1996).

[9] T. Bollerslev, J. Econometr. **31**, 307 (1986).

[10] *Handbook of Mathematical Functions*, edited by M. Abramowitz and I. A. Stegun (Dover, New York, 1972).

[11] E. Koscielny-Bunde, A. Bunde, S. Havlin, H.E. Roman, Y. Goldreich, and H.J. Schellnhuber, Phys. Rev. Lett. **81**, 729 (1998).